J. Agr. Sci. Tech. (2016) Vol. 18: 1781-1792

Enhancement of Thermal Stability and Antioxidant Activity of Thyme Essential Oil by Encapsulation in Chitosan Nanoparticles

M. Ghaderi Ghahfarokhi[1], M. Barzegar[1*], M. A. Sahari[1], and M. H. Azizi[1]

ABSTRACT

The use of essential oils as the preservative agents in food industry faces the problem of interactions with food matrix components, low solubility in aqueous phase, high volatile character and sensitivity to environmental conditions. The aim of this study was to enhance thermal stability and antioxidant activity of Thyme essential Oil (TO) by encapsulation in Chitosan Nanoparticles (CS-NP). TO was encapsulated in CS-NP with an emulsion–ionic gelation crosslinking method and the construction was confirmed by Fourier Transform Infrared spectroscopy (FT-IR) and thermogravimetric analysis techniques. The effect of CS: TO weight ratio encapsulation efficiency, loading capacity, particle size and zeta potential of TO-loaded Chitosan Nanoparticle (CS-NP-TO) were investigated. The encapsulated TO was decomposed at a higher temperature (318-325.4ºC) than free TO (170ºC) reflecting the enhanced thermal stability of TO by encapsulation. Also, when TO was encapsulated in CS-NP, antioxidant activity proved to be superior from that of free TO. The considerable antioxidant activity and thermal stability reveal that such particles have promising application for delivery of TO in medicine, food and feed.

Keywords: Antioxidant activity, Chitosan nanoparticle, Encapsulation, Thermal stability, Thyme oil.

INTRODUCTION

Due to increasing pressure from consumers or legal authorities on toxicological concerns of synthetic additives**,** growing attention has been paid to natural substances with beneficial health properties for application as a food preservative, nutraceutical and medicine (Tao *et al.,* 2014). Essential Oils (EOs) are secondary metabolites of aromatic plants. They are obtained from different plant materials. Many of EOs are categorized by the FDA and generally recognized as safe (Hyldgaard *et al.,* 2012).

Thymus vulgaris L. (common thyme) is an aromatic/medicinal plant that belongs to the genus *Thymus* of Lamiaceae family (Morales, 2002). Thyme has been employed in medicine, food, agriculture, veterinary and pest control (Tao *et al.,* 2014). Nevertheless, the use of EOs as the preservative agents in food industry still faces the problem of interactions with food matrix components such as fat, protein and starch (Hyldgaard *et al.,* 2012), low solubility in aqueous phase, alteration of sensorial characteristics of foodstuff at high concentration (Weiss *et al.,* 2009; Tao *et al.,* 2014), sensitivity to oxygen, light and heat during processing, utilization and storage (Woranuch and Yoksan, 2013) and high volatile character (Hosseini *et al.,* 2013; Khalili *et al.,* 2015).

Nanoencapsulation is defined as a technology to encapsulate substances in miniature and refers to bioactive packing at the nano-scale range (Lopez-Rubio *et al.,* 2006). Encapsulation of EOs can possibly solve challenges facing their applications by

[1] Department of Food Science and Technology, Faculty of Agriculture, Tarbiat Modares University, Tehran, P. O. Box: 14115-336, Islamic Republic of Iran.
[*] Corresponding author; e-mail: mbb@tmu.ac.ir

[Downloaded from jast.modares.ac.ir on 2024-10-12]

[DOR: 20.1001.1.16807073.2016.18.7.20.0]

enhancing bioavailability and solubilization, protecting from chemical and thermal degradation and controling the delivery at the desired time and site (Tao *et al.*, 2014). Chitosan (CS) has been widely considered as a versatile polymer in development of micro and nano encapsulation system as a wall material because of remarkable properties including biocompatibility, biodegradability and low toxicity (Jang and Lee, 2008; Ajun *et al.*, 2009). CS is a natural polysaccharide comprising copolymers of glucosamine and N-acetyl glucosamine, soluble in acidic media and exists as linear cationic chains when its amino groups are protonated (Wilson *et al.*, 2010). As a widely used method for preparing Chitosan Nanoparticles (CS-NP), ionotropic gelation is based on the electrostatic interaction of positively charged CS chains with specific polyanions such as tripolyphosphate to form inter and intra molecular cross-linkages under the acidic condition (Fan *et al.*, 2012).

CS-NPs have been extensively studied in pharmaceutics and food application for encapsulation of drug and plant-derived bioactive compounds. Based on our knowledge up to now there has been no study on entrapment of TO into CS-NPs prepared by emulsion-gelation technique. The aim of this study was to enhance thermal stability and antioxidant activity of Thyme essential Oil (TO) by encapsulation in CS-NP (by the emulsion-gelation method). The physicochemical characteristics of CS-NP-TO along with antioxidant activity of TO were also investigated.

MATERIALS AND METHODS

Materials

Chitosan (75–85% degree of deacetylation and M_w= 760 kDa), penta sodium TriPolyPhosphate (TPP) and 1, 1-DiPhenyl-2-PicrylHydrazyl (DPPH), were purchased from Sigma–Aldrich Chemical Co. (St. Louis, USA). Tween 80 was supplied by Loba chemie (Mumbai, India) and acetic acid glacial and sodium acetate were prepared from Rankem (New Delhi, India). Thyme essential oil (*Thymus vulgaris* L.) was purchased from Giah Essence Phytopharm Co. (Gorgan, Iran) and ultrapure water (denoted as dd. H_2O) was prepared with the Purise system (Seoul, South Korea).

Encapsulation of Thyme Oil in Chitosan Nanoparticle

The CS-NP and CS-NP-TO were prepared by two-steps process: Oil-in-Water (O/W) emulsification and ionic gelation according to the modified methods of Jang and Lee (2008) and Keawchaoon and Yoksan (2011). Chitosan solutions (3.2 mg ml^{-1}) were prepared by dissolving chitosan in acetic acid followed by 60 minutes sonication (ULTRASONS-H, Selecta, Spain) until the solution became transparent. Then, chitosan solution was filtered through 1µm pore size filter in order to eliminate any undissolved chitosan. The pH of the solutions was adjusted to 4 using NaOH solution (5N). Tween-80 (80 mg) was added as a surfactant to the solution (50 ml) and stirred at 60°C for 30 minutes to gain a homogeneous mixture. Various amounts of TO (0.0, 32, 64, 96 and 128 mg) were dissolved separately in 4 ml ethanol to obtain different weight ratios of chitosan to TO of 1:0, 1:0.2, 1:0.4, 1:0.6 and 1:0.8, respectively. After cooling, oil phase was gradually dropped into the aqueous phase under stirring vigorously for 4 min and agitation was continued for 20 min. Subsequently, 30 ml of TPP solution (1.87 mg ml^{-1}) with equal pH was added drop wise into aqueous solution for 30 minutes using magnetic stirrer. To ensure complete gelation, mixing was continued for 30 minutes after the complete addition of the TPP.

Morphological and Physiochemical Characterization of Nanoparticles

The Z-average diameter, PDI and zeta potential of freshly prepared CS-NP and CS-

[Downloaded from jast.modares.ac.ir on 2024-10-12]

[DOR: 20.1001.1.16807073.2016.18.7.20.0]

NP-TO were determined using Malvern Zetasizer Nano ZS (Malvern Instruments Ltd., Malvern, UK) equipped with an He–Ne laser operating at 4.0 mW and 633 nm with a fixed scattering angle of 90°. All samples were measured in triplicate.

The chemical structures of chitosan powder, TO, freeze-dried CS-NP and CS-NP-TO were acquired at 4000-400 cm^{-1} using a Nicolet IR100 FTIR spectrometer (Thermo, USA) with 4 cm^{-1} resolution.

The thermal stability of the TO and freeze dried CS-NP and CS-NP-TO were investigated using thermogravimetric analysis. Thermal Gravimetric Analysis (TGA)/Derivative Thermal Gravimetric (DTG) analysis was carried out with TGA/DSC 1 Stare System (Mettler Toledo, Switzerland) from 25 to 600°C with a heating rate of 10°C min^{-1} under nitrogen atmosphere with a flow rate of 50 cm^3 min^{-1}.

Scanning electron microscopy (SEM, KYKY- EM3200, China) was used for morphological characterization of CS-NP and CS-NP-TO (with CS: TO ratio of 1:0.4). One ml of nanoparticle suspension was diluted in 50 ml of double distilled water and then sonicated for 1 min in ultrasonic bath (Selecta ULTRASONS, Spain). 50 µl of the dilution was deposited on a cleaned glass surface and dried under vacuum at 30°C (VO 200, Memmert, Germany). Dried nanoparticles were coated with gold metal using sputter coater (KYKY-SBC12, China) before being observed on SEM.

Determination of Encapsulation Efficiency (EE) and Loading Capacity (LC)

The Encapsulation Efficiency (EE) of the CS-NP-TO was determined by the separation of nanoparticles from the aqueous medium containing free TO. The amount of TO in the supernatant was determined by a spectrophotometer (Cary 60, Agilent, US) at 274 nm. Loading capacity (LC) of CS-NP-TO was determined by Thermogravimetric (TGA/DTG) technique. The EE and LC of CS-NP-TO were calculated using the following equations:

$$\%EE = \frac{(Total\ amount\ of\ TO - Initial\ amount\ of\ TO) \times 100}{Initial\ amount\ of\ TO}$$

Evaluation of Antioxidant Activity

The capacity of the free and encapsulated TO to scavenge the free radical 1, 1-DiPhenyl-2-PicrylHydrazyl (DPPH) was assessed according to the slightly modified method of Hatano *et al.* (1988). Briefly, various amounts of CS-NP-TO (prepared with CS:TO weight ratio of 1:0.8) were dispersed in ethanol (99%) to obtain final concentrations of 0.1-1 mg ml^{-1} of TO. Samples were stirred for 4 hours at 200 rpm to release TO from CS-NPs. In the case of free TO and CS-NP, the solutions with similar concentration (0.1-1 mg ml^{-1}) were made in ethanol. Then, 0.3 ml of various concentration of TO (free and encapsulated) and CS-NP in ethanol was added to 2.7 ml of the ethanolic solution (6×10-5 mol L^{-1}) of DPPH. The mixture was shaken and incubated for 30 minutes at room temperature in the dark. After incubation, the samples of CS-NP-TO and CS-NP were ultracentrifuged at 24,000 rpm for 5 minutes to obtain a clear supernatant for analysis. Then the absorbance of the mixture was measured at 517 nm against a blank (ethanol) using UV-Vis spectrophotometer. A mixture consisting of 0.3 ml of ethanol and 2.7 ml of DPPH solution was used as the control. The inhibition percentage was calculated according to the following formula:

$$\%LC = \frac{(\text{Amount of loaded TO}) \times 100}{\text{Weight of sample}}$$

here, *Ac* and *As* are the absorbance values of the control and of the sample, respectively. The experiment was carried out in triplicate.

[Downloaded from jast.modares.ac.ir on 2024-10-12]

[DOR: 20.1001.1.16807073.2016.18.7.20.0]

RESULTS AND DISCUSSION

Characterization of Thyme Oil, CS-NP and CS-NP-TO

The volatile oils are complex mixture systems and the IR spectra displays a total overlap of each absorption spectrum of various compounds. The TO used in this study contained significant quantities of thymol and carvacrol (11.0 and 21.3%, respectively). Several characteristic bands can be extracted from FTIR spectra of free TO (Figure 1-a), such as 3,525 (OH vibration of hydroxyl group of thymol), 2,962 (C-H stretching of methyl and isopropyl groups on the phenolic rings of thymol), 1,619 (conjugated double bond of the ring), 1581 (NH bending), 1,511 (C=C aromatic ring), 1,457 (CH deformation), 1288 (C-O-C stretching) and 809 cm^{-1} (out-of-plane CH wagging vibrations). According to the former study on the individual essential oil components (Schulz *et al.*, 2003), in the FTIR spectra of the TO, only the characteristic peaks of thymol were observed (2962, 1619, 944 and 809 cm^{-1}) and the evidence of the investigated TO was the thymol-type. The characteristic signals of CS were O-H and N-H stretching around 3,500–3,200 cm^{-1}. In addition, C-H stretching (2,922 cm^{-1}), amide I (1,643 cm^{-1}), C-O-C stretching (1085 cm^{-1}) and pyranoside ring stretching vibration (894 cm^{-1}) were also found. The band located at 1,378 cm^{-1} is assigned to the acetamide groups, indicating that CS is not completely deacetylated (Figure 1-b). The spectrum of CS-NP (Figure 1-c) shows some differences with CS powder that implies the NP formation. In CS-NP the peak of 3,439 cm^{-1} shifted to a lower wavenumber (3,409 cm^{-1}) and becomes wider, indicating that hydrogen

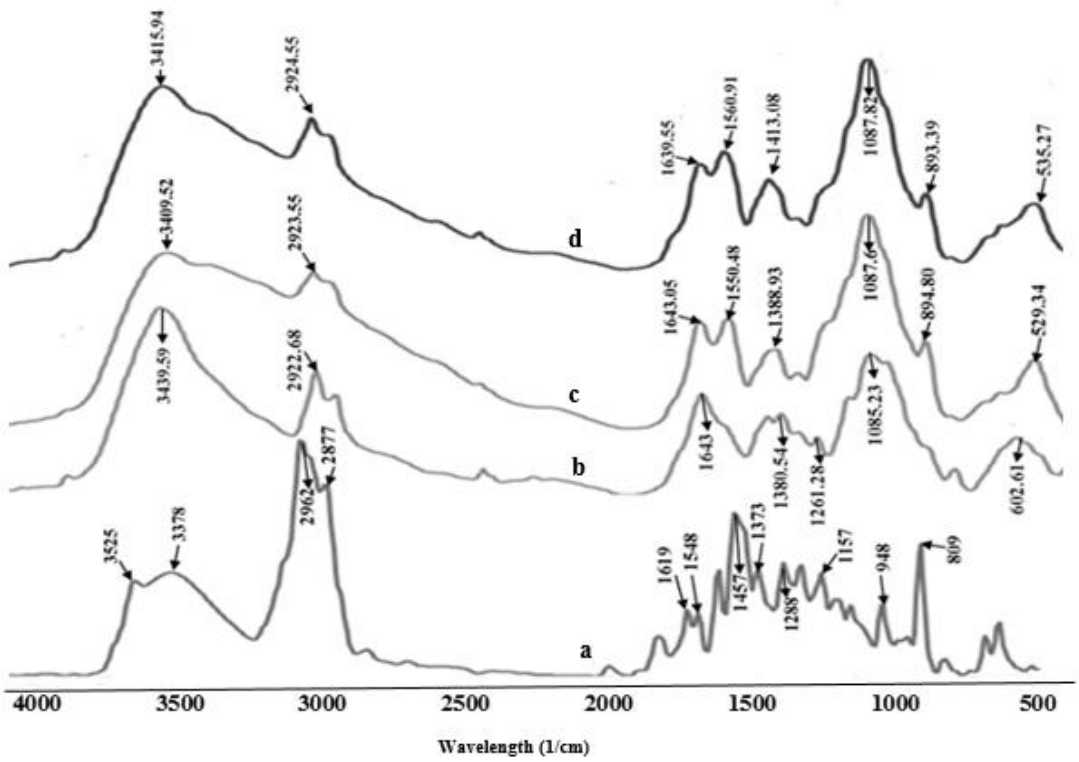

Figure 1. FTIR spectra of: (a) Thyme essential oil; (b) Chitosan powder; (c) Chitosan nanoparticle, and (d) Thyme oil loaded chitosan nanoparticle with chitosan: Thyme essential oil weight ratio of 1:0.4.

[Downloaded from jast.modares.ac.ir on 2024-10-12]

[DOR: 20.1001.1.16807073.2016.18.7.20.0]

bonding between CS and TPP is enhanced. Moreover, new peaks appeared at 1,550 cm^{-1} (amide II) which could be ascribed to the electrostatic interaction between phosphoric groups of TPP and NH_3^+ ions. These results are consistent with earlier report for CS and CS-NP (Jingou *et al.*, 2011). Most of the specific peaks of TO disappeared when it was loaded in CS-NP (Figure 1-d). The absence of new peaks in the CS-NP-TO reflected that the TO and CS are physically attached to each other without any chemical interaction. The incorporation of TO into CS-NP caused shifts and flattening in the peaks associated with the O-H and N-H stretching (3,400 cm^{-1}). These shifts may be resulted from interactions between molecules without the formation of covalent bonds e.g. hydrogen bonds, hydrophobic forces, and electrostatic interactions (Davidov-Pardo *et al.*, 2015). These results are in good agreement with those reported previously by Hosseini *et al.* (2013) who reported no chemical interaction or modifications were seen in FT-IR spectra of oregano oil loaded-CS-NP.

TGA is a useful analytical technique to monitor the weight loss of a material as a function of temperature or time. The decomposition Temperature (T_d) is the temperature corresponding to the maximum slopes of each weight change step. The T_d is obviously seen as a peak when the rate of mass loss with respect to temperature, a so-called Derivative ThermoGravimetry (DTG) thermogram, is plotted. TG/DTG curve profiles revealed the decrease in weight of TO, CS-NP and CS-NP-TO with increasing the temperature from 100 to 600ºC (Figures 2-a and -b). The TG/DTG profile of TO showed only one evaporation stage and a quick mass loss as a function of temperature. The mass loss of TO begins at temperatures around 74.13°C (Figure 2-a) with a peak at 170ºC (Figure 2-b). CS-NP-TO samples exhibit similar thermal degradation behaviors which are different from CS-NP. CS-NP and all CS-NP-TO samples show the presence of two (Figure 2-a) and three (Figure 2-b) thermal events, respectively. The first weight loss event appeared below 100°C for all particles. The weight loss at these temperature ranges is primarily attributed to the evaporation of adsorbed and bound moisture. The second event for CS-NP and CS-NP-TO is due to the dehydration of the saccharide rings, depolymerization and decomposition of the acetylated and deacetylated units of the CS (Peniche-Covas *et al.*, 1993), which compose the nanoparticle wall material. Thermal degradation Temperatures (T_d) for decomposition of CS in different samples are given in Figure 2-b. In addition to the aforesaid, CS-NP-TO showed a two-step mass loss when a low content of TO (CS:TO

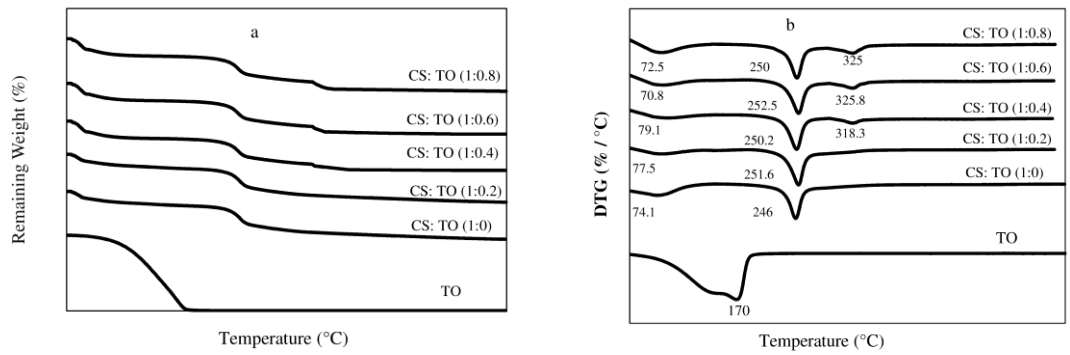

Figure 2. (a) TGA, and (b) DTG thermograms of Thyme essential Oil (TO), Chitosan Nanoparticle (CS-NP) and Thyme Oil loaded Chitosan Nanoparticle (CS-NP-TO) prepared using different initial weight ratios of Chitosan: Thyme essential Oil (CS:TO).

[Downloaded from jast.modares.ac.ir on 2024-10-12]

[DOR: 20.1001.1.16807073.2016.18.7.20.0]

ratio of 1:0.2, Figure 2-b) was loaded and at high content of TO, loaded particle showed new T_d ranging from 318.3- 325.8 °C which corresponded to the loss of encapsulated TO. The weight loss at this temperature was then used to compute the content of loaded TO in CS-NP-TOs. Results revealed the attainment of TO loading into CS-NP. It was noted that the encapsulated TO was decomposed at a higher temperature than its free form, reflecting the enhanced thermal stability of TO by encapsulation. This phenomenon can be explained by some hydrophobic–hydrophilic interactions between the wall material and essential oil reported for encapsulation of oregano essential oil loaded microparticles (Hijo *et al.*, 2015). A similar result was obtained by Woranuch and Yoksan (2013), reporting that the thermal stability of eugenol increased through encapsulation into CS-NP.

Shape, Size, PDI and Zeta Potential of CS-NP and CS-NP-TO

Particle size, surface charge, and *PDI* are momentous considerations for designing delivery system of bioactive compounds. In theory, the ideal characteristics of NPs are the smallest size, highest surface charge and lowest *PDI* (Bulmer *et al*., 2012). Particle size is one of the most important considerations of NPs which determine their mucosal and epithelial tissue uptake and the intracellular trafficking (Panyam and Labhasetwar, 2003). *PDI* is an indicator of dispersion homogeneity and varied from 0 to 1 (Zhang and Kosaraju, 2007). Uniform particle size distribution is crucial in maintaining a constant drug release rate and hence should be minimized. Dynamic Light Scattering (DLS) was used to determine the particle size, zeta potential and PDI of fresh dispersions of CS-NP-TO. In general, the CS-NO-TO experienced a decrease in size with increasing CS:TO weight ratio (Table 1). Size of the formed nanoparticles decreased from 215.43±0.48 nm for the 1:0 ratio to 121.03±4.45 nm for 1:0.8 ratio. Since the size measured by the DLS technique might be the hydrodynamic diameters of aggregate particles and/or hydrated individual particles, the results reflected that the aggregation and/or swelling of CS-NP-TO in aqueous medium were lower than those of CS-NP. This might be explained by the hydrophobicity of TO entrapped inside or on the surface of particles. A similar phenomenon was also reported for encapsulation of ascorbyl palmitate (Yoksan *et al*., 2010) and *Zataria multiflora* essential oil (Mohammadi *et al.*, 2015) in CS-NPs. The particle size of the CS-NPs loaded with carvacrol (Keawchaoon and Yoksan, 2011) ranged between 518.5-716.8 nm, respectively. Smaller particle size in our study can be correlated with different degradation mechanisms of chitosan molecules. Cavitation effect of ultrasonic radiation used for CS-NP-TO preparation fragmented the long chains of CS to smaller pieces and prevented the formation of large nanoparticles. CS-NP-TO showed *PDI* in the range of 0.388-0.451. Size and size distribution of the CS-NP, prepared with ionic gelation method, was influenced mainly by concentration, molecular weight and mixing method (by stirrer or sonicator). The wide size distribution may be originated from chitosan's broad range of molecular weight; chitosan has different molecular weights (low, medium and high) and distribution size (Gan *et al.*, 2005).

The nature and amount of the surface charge, expressed as zeta potential, is a major characteristic of NPs as it influences their interaction with the surrounding environment and bioactive constitutes (Cho *et al.*, 2013). The surface charge of prepared CS-NP-TOs at different CS:TO ratios, were determined by zeta potential measurement. CS-NPs showed a zeta potential value of +35.35±0.4 mV implying a positively charged surface of the particles (Table 1). As the initially loaded concentration of TO increased, the zeta potential significantly decreased to values ranging from +30.67±0.3 to +22.9 ±0.1 mV. This result may be explained by adsorption of TO on

[Downloaded from jast.modares.ac.ir on 2024-10-12]

[DOR: 20.1001.1.16807073.2016.18.7.20.0]

Table 1. Particle size, zeta potential, *PDI*, Encapsulation Efficiency (EE) and loading capacity (LC) of CS-NP and CS-NP-TO prepared with different ratios of CS TO.[a]

CS:TO ratio	*EE* (%)	*LC* (%)	Particle size (nm)	Zeta potential (mV)	*PDI*
1 : 0	0	0	215.43 ± 0.484	+ 35.35 ± 0.4	0.433±0.005
1 : 0.2	42.16±0.16	Nd	194.7 ± 0.838	+ 30.67 ± 0.3	0.451±0.023
1 : 0.4	36.20±0.91	5.62	185.13 ± 1.05	+ 27.8 ± 0.1	0.448±0.02
1 : 0.6	26.84±0.70	6.35	131.06 ± 1.55	+ 25.7 ± 0.2	0.415±0.021
1 : 0.8	30.67±1.62	7.55	121.03 ± 4.45	+ 23.0 ± 0.1	0.388±0.018

[a] Results were reported as mean±*SD* (n= 3). *PDI*: PolyDispersity Index; CS-NP: Chitosan Nanoparticle; CS-NP-TO: Thyme Oil loaded Chitosan Nanoparticle, Nd: Not determined.

the surface of CS-NP-TO particles. This finding was in agreement with the previous report for ammonium glycyrrhizinate (Wu *et al.*, 2005).

The morphological observation of CS-NP and CS-NP-TO (at CS:TO ratio of 1:0.4) was performed by SEM technique after cast drying of samples suspension on a glass surface under vacuum. For CS-NP, the aggregation of particles was visible (Figures 3-a and -b). The SEM photographs of the prepared CS-NP-TO revealed that nanoparticles were almost spherical in shape with regular distribution (Figures 3-c and -d). These observations are also in agreement with the spherical particles produced after the encapsulation of *Mentha piperita* essential oil within chitosan-cinnamic acid

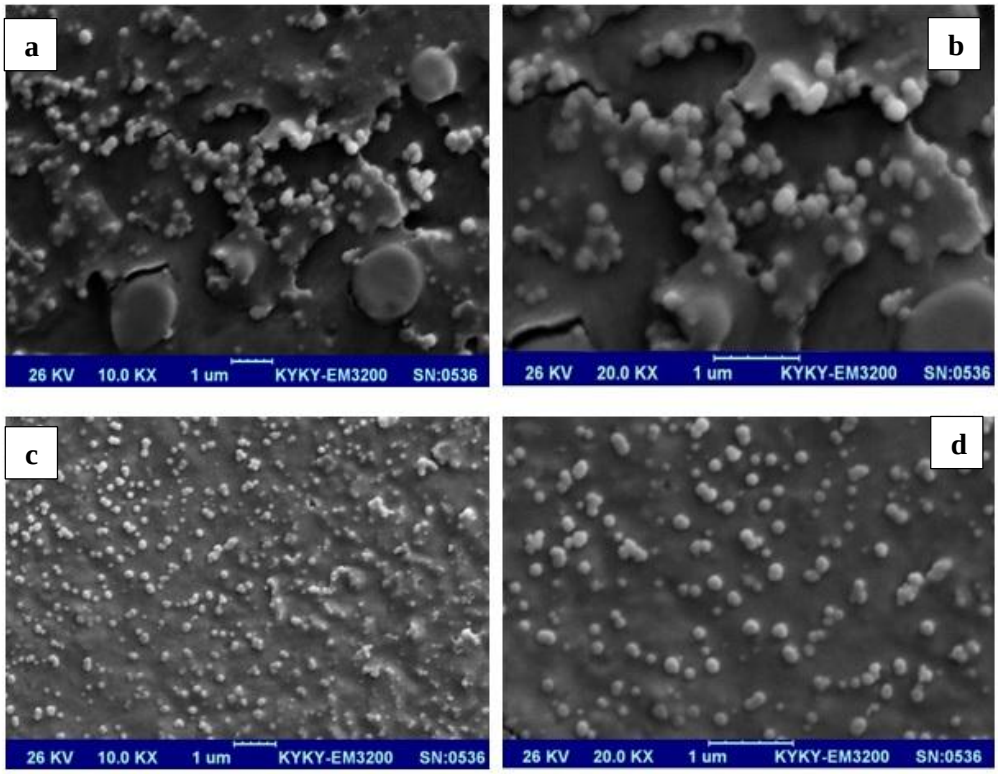

Figure 3. SEM image at 26 kV of: (a) Chitosan nanoparticle (10,000X); (b) Chitosan nanoparticle (20,000X); (c) Thyme essential oil loaded chitosan nanoparticle prepared using an initial weight ratio of chitosan: thyme essential oil of 1: 0.4 (10,000X), and (d) 1: 0.4 (20,000X).

[Downloaded from jast.modares.ac.ir on 2024-10-12]

[DOR: 20.1001.1.16807073.2016.18.7.20.0]

nanogel (Beyki *et al.*, 2014). The size measured by the SEM technique (66.6-152.5 nm) was lower than the size measured by DLS method and it might be an effect of swilling and aggregation of the nanoparticles during dispersion in water (Esmaeili and Asgari, 2015).

Encapsulation Efficiency and Loading Capacity

To evaluate the *EE*, calibration curve of TO in ethanol was prepared and the amount of TO within and outside of the developed CS-NP-TO was then monitored by using UV–Vis technique. Encapsulation efficiency is defined as the percentage of initial TO content that can be entrapped into CS-NP. As seen in Table 1, *EE* of the CS-NP-TO were affected by the initial CS:TO weight ratio. This result could indicate that the *EE* tended to decrease upon increasing the initial TO content and decreasing in particle size. Percent of *EE* of the produced loaded capsules were over the range 42.2-26.8% which the CS:TO weight ratio of 1:0.2 showed maximum *EE*. One potential explanation is saturation of TO loading into CS-NP with increasing concentration. Therefore, the excess essential oil was weakly absorbed on the surface of the particles and easily detached during the collection of the CH-NP-TOs by centrifugation. Our results are in accordance with previous research showing reversed linear correlation between encapsulation efficiency and vitamin C (Alishahi *et al.*, 2011) concentration. Also, Jang and Lee (2008) reported that the low encapsulation efficiency of the ascorbic acid loaded nanoparticle was related to weak interaction between ascorbic acid and chitosan nanoparticles.

Furthermore, data obtained from TGA thermogram was employed to determine the *LC* (%) of CS-NP-TOs (Table 1). As mentioned earlier, a new range of weight loss appeared at temperatures ranging from 235-293°C in the TGA thermogram of CS-NP-TOs, corresponding to the T_d of encapsulated TO. The percent weight loss at this temperature range was used to calculate the content of TO. Based on the TAG result, the *LC*% of TO was in a range of 5.62-7.55%. The augmentation of *LC* and reduction of EE as a function of CS:TO weight ratio corresponded to a previous study related to the loading of aspirin into CS-NP (Ajun *et al.*, 2009).

Antioxidant Activity of Free and Encapsulated TO

The DPPH radical scavenging assay is an advantageous method for the assessment of the antioxidant effectiveness of different substances. DPPH is a stable radical with purple color at room temperature that turns to yellow followed by reduction in the presence of an antioxidant compound (Huang *et al.*, 2005). The scavenging effect of free and encapsulated TO on DPPH radicals showed a concentration-dependent activity (Figure 4) and being in the range of 17.2-53.4 and 23.7-64.54%, respectively. The antioxidant activity of samples was also expressed as IC50 which was defined as the concentration (in mg ml^{-1}) of TO required to scavenge DPPH radicals by 50%. The *IC50* value of the encapsulated TO (0.65 mg ml^{-1}) was lower than that of free TO (0.86 mg ml^{-1}) indicating that free radical scavenging activity of TO improved by 24.45% after entrapment in the CS-NPs. This might be interpreted by the fact that the protective effect of encapsulation decreases evaporation rate via controlled release of TO during assay. Our results were in accordance with those obtained by Woranuch and Yoksan (2013) who reported a similar enhanced antioxidant activity for encapsulated eugenol in nanoparticles compared to free eugenol. In addition, in previous studies, it has been showed that the antioxidant activity of astaxanthin was effectively maintained in linoleic acid system after encapsulation in calcium alginate gel beads compared to the same amount of non-encapsulated

[Downloaded from jast.modares.ac.ir on 2024-10-12]

[DOR: 20.1001.1.16807073.2016.18.7.20.0]

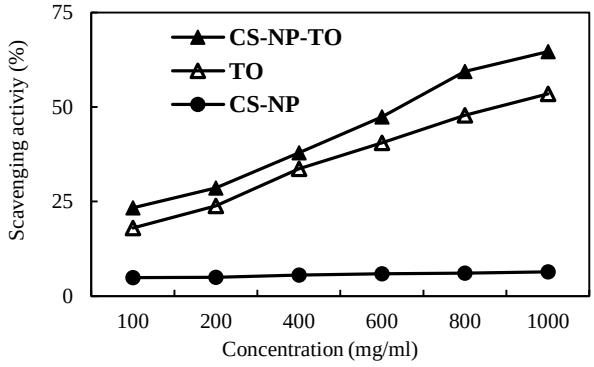

Figure 4. DPPH scavenging activity (%) of free Thyme essential Oil (TO) and Thyme Oil loaded Chitosan Nanoparticles (CS-NP-TO) prepared using an initial weight ratio of chitosan: thyme essential oil of 1: 0.8.

astaxanthin (Lee *et al.*, 2011). Antioxidant activity of chitosan chains is related to hydroxyl and amino groups that can react with free radicals. CS-NP showed low scavenging activity (4.9-6.4%) at investigated concentration because of cross-linking between amino group of chitosan and TPP polyanion (Xie *et al.*, 2001).

CONCLUSIONS

In the present study, CS-NP and CS-NP-TO was successfully prepared under mild conditions by emulsion-gelation method. The fundamental characteristics of the CS-NP-TOs including particle size, zeta potential and encapsulation efficiency were strongly dependent on the CS: TO ratio and 1: 0.8 ratio was better than the others. Encapsulated TO showed a greater radical scavenging activity than free TO. Encapsulation of EOs with natural polymers enhances their biological activity and overcomes the problems relating to low stability and poor water solubility for efficient utilization in food systems.

ACKNOWLEDGEMENTS

This work was performed with the support of Tarbiat Modares University Research Council.

REFERENCES

1. Ajun, W., Yan, S., Li, G. and Huili, L. 2009. Preparation of Aspirin and Probucol in Combination Loaded Chitosan Nanoparticles and *In vitro* Release Study. *Carbohydr. Polym.*, **75**: 566–574.
2. Alishahi, A., Mirvaghefi, A., Tehrani, M. R., Farahmand, H., Shojaosadati, S. A., Dorkoosh, F. A. and Lsabee, M. Z. 2011. Shelf Life and Delivery Enhancement of Vitamin C Using Chitosan Nanoparticles. *Food Chem.*, **126:** 935–940.
3. Barbosa-Cánovas, G., Mortimer, A., Lineback, D., Spiess, W., Buckle, K. and Colonna, P. 2009. Global Issues in Food Science and Technology, In: "*Nanostructured encapsulation systems: food antimicrobials*" (Eds.): Weiss, J., Gaysinsky, S., Davidson, M. and McClements, J., Academic Press. New York, PP. 425-479.
4. Beyki, M., Zhaveh, S., Khalili, S. T., Rahmani-Cherati, T., Abollahi, A., Bayat, M., Tabatabaei, M. and Mohsenifar, A. 2014. Encapsulation of *Mentha piperita* Essential Oils in Chitosan-cinnamic Acid Nanogel with Enhanced Antimicrobial Activity against *Aspergillus flavus. Ind. Crops Prod.*, **54:** 310–319.
5. Bulmer, C., Margaritis, A. and Xenocostas, A. 2012. Production and Characterization of Novel Chitosan Nanoparticles for Controlled

[Downloaded from jast.modares.ac.ir on 2024-10-12]

[DOR: 20.1001.1.16807073.2016.18.7.20.0]

Release of rHu-Erythropoietin. *Biochem. Eng. J.*, **68:** 61-69.
6. Cho, E. G., Holback, H., Liu, K. C., Abouelmagd, S. A., Park, J. and Yeo, Y. 2013. Nanoparticle Characterization: State of the Art, Challenges and Emerging Technologies. *Mol. Pharmacol.*, **10:** 2093-2110.
7. Davidov-Pardo, G., Joye, I. G. and McClements, D. J. 2015. Encapsulation of Resveratrol in Biopolymer Particles Produced Using Liquid Antisolvent Precipitation. Part 1. Preparation and Characterization. *Food Hydrocol.*, **45:** 309-316.
8. Esmaeili, A. and Asgari, A. 2015. *In vitro* Release and Biological Activities of *Carum copticum* Essential Oil (CEO) Loaded Chitosan Nanoparticles. *Int. J. Biol. Macromol.*, **81**: 283-290.
9. Fan, W., Yan, W., Xu, Z. and Ni, H. 2012. Formation Mechanism of Monodisperse, Low Molecular Weight Chitosan Nanoparticles by Ionic Gelation Technique. *J. Coll. Surf. B Biointerfaces*, **90:** 21-27.
10. Gan, Q., Wang, T., Cochrane, C. and McCarron, P. 2005. Modulation of Surface Charge, Particle Size and Morphological Properties of Chitosan–TPP Nanoparticles Intended for Gene Delivery. *J. Coll. Surf. B Biointerfaces*, **44:** 65-73.
11. Hosseini, S. F., Zandi, M., Rezaei, M. and Farahmandghavi, F. 2013. Two-step Method for Encapsulation of Oregano Essential Oil in Chitosan Nanoparticles: Preparation, Characterization and *In vitro* Release Study. *J. Carbohydr. Polym.*, **95:** 50–56.
12. Hatano, T., Kagawa, H., Yasuhara, T. and Okuda, T. 1988. Two New Flavonoids and Other Constituents in Licorice Root: Their Relative Astringency and Scavenging Effects. *Chem. Pharm. Bull.*, **36:** 2090–2097.
13. Hijo, A. A. C. T., Campos, A. A., Costa, J. M. G., Silva, E. K., Azevedo, V. M., Yoshida, M. I. and Borges, S. V. 2015. Physical and Thermal Properties of Oregano (*Origanum vulgare* L.) Essential Oil Microparticles. *J. Food Process. Eng.*, **38**: 1-10.
14. Huang, D. J., Ou, B. X. and Prior, R. L. 2005. The Chemistry Behind Antioxidant Capacity Assays. *J. Agric. Food Chem.*, **53:** 1841-1856.
15. Hyldgaard. M., Mygind, T. and Meyer, R. L. 2012. Essential Oils in Food Preservation: Mode of Action, Synergies, and Interactions with Food Matrix Components. *Front Microbiol.*, **3:** 1-24.
16. Jang, K. I. and Lee, H. G. 2008. Stability of Chitosan Nanoparticles for *L*-Ascorbic Acid during Heat Treatment in Aqueous Solution. *J. Agric. Food Chem.*, **56:** 1936-1941.
17. Jingou, J., Shilei, H., Weiqi, L., Danjun, W., Tengfei, W. and Yi, X. 2011. Preparation, Characterization of Hydrophilic and Hydrophobic Drug in Combine Loaded Chitosan/Cyclodextrin Nanoparticles and *In vitro* Release Study. *J. Coll. Surf. B Biointerfaces*, **83:** 103–107.
18. Keawchaoon, L. and Yoksan, R. 2011. Preparation, Characterization and *In vitro* Release Study of Carvacrol-loaded Chitosan Nanoparticles. *J. Coll. Surf. B Biointerface.*, **84:** 163-171.
19. Khalili, S.T., Mohsenifar, A., Beyki, M., Zhaveh, S., Rahmani-Cherati, T., Abdollahi, A., Bayat, M. and Tabatabaei, M. 2015. Encapsulation of Thyme Essential Oils in Chitosan-benzoic Acid Nanogel with Enhanced Antimicrobial Activity against *Aspergillus flavus. LWT-Food Sci. Technol.*, **60:** 502-508.
20. Lee, J. S., Park, S. A., Chung, D. and Lee, H. G. 2011. Encapsulation of Astaxanthin-rich *Xanthophyllomyces dendrorhous* for Antioxidant Delivery. *Int. J. Biol. Macromol.*, **49:** 268-273.
21. Lopez-Rubio, A., Gavara, R. and Lagaron, J. 2006. Bioactive Packaging: Turning Foods into Healthier Foods through Biomaterials. *Trend. Food Sci. Technol.*, **17:** 567–575.
22. Mohammadi, A., Hashemi, M. and Hosseini, S. M. 2015. Nanoencapsulation of *Zataria multiflora* Essential Oil Preparation and Characterization with Enhanced Antifungal Activity for Controlling *Botrytis cinerea*, the Causal Agent of Gray Mould Disease. *Innov. Food Sci. Emerg, Technol.*, **28:** 73-80.
23. Morales, R. 2002. Medicinal and Aromatic Plants Industrial Profiles, In: "*The History, Botany and Taxonomy of the Genus Thymus*", (Eds.): Stahl-Biskup, E. and Saez, F. Taylor Francis, London, PP. 1–44.
24. Panyam, J. and Labhasetwar, V. 2003. Biodegradable Nanoparticles for Drug and Gene Delivery to Cells and Tissue. *Adv. Drug Delivery Rev.*, **55:** 329-347.

[Downloaded from jast.modares.ac.ir on 2024-10-12]

[DOR: 20.1001.1.16807073.2016.18.7.20.0]

25. Peniche-Covas, C., Arguelles-Monal, W. and Rom, J. S. 1993. A Kinetic Study of the Thermal Degradation of Chitosan and a Mercaptan Derivative of Chitosan. *Polym. Degrad. Stabil.*, **39:** 21–28.
26. Schulz, H., Quilitzsch, R. and Kruger, H. 2003. Rapid Evaluation and Quantitative Analysis of Thyme, Oregano and Chamomile Essential Oils by ATR-IR and NIR Spectroscopy. *J. Mol. Struct.*, **661-662:** 299-306.
27. Tao, F., Hill, L. E., Peng, Y. and Gomes, G. L. 2014. Synthesis and Characterization of *β*-Cyclodextrin Inclusion Complexes of Thymol and Thyme Oil for Antimicrobial Delivery Applications. *LWT- Food Sci. Technol*., **59:** 247-255.
28. Wilson, B., Samanta, M. K., Santhi, K., Kumar, K. P. S., Ramasamy, M. and Suresh, B. 2010. Chitosan Nanoparticles as a New Delivery System for the Anti-Alzheimer Drug Tacrine. *Nanomed. Nanotech. Biol Med*., **6:** 144-152.
29. Woranuch, S. and Yoksan, R. 2013. Eugenol-loaded Chitosan Nanoparticles. I. Thermal Stability Improvement of Eugenol through Encapsulation. *J. Carbohydr. Polym*., **96:** 578– 585.
30. Wu, Y., Yang, W., Wang, C., Hu, J. and Fu, S. 2005. Chitosan Nanoparticles as a Novel Delivery System for Ammonium Glycyrrhizinate. *Int. J. Pharm.*, **295:** 235–245.
31. Xie, W., Xu, P. and Liu, Q. 2001. Antioxidant Activity of Water-soluble Chitosan Derivatives. *Bioorg. Med. Chem. Lett*., **11:** 1699-1701.
32. Yoksan, R., Jirawutthiwongchai, J. and Arpo, K. 2010. Encapsulation of Ascorbyl Palmitate in Chitosan Nanoparticles by Oil-in-water Emulsion and Ionic Gelation Processes. *Coll. Surf. B: Biointerfaces*, **76:** 292-297.
33. Zhang, L. and Kosaraju, S. L. 2007. Biopolymeric Delivery System for Controlled Release of Polyphenolic Antioxidants. *Eur. Polym. J*., **43:** 2956–2966.

افزایش ثبات حرارتی و فعالیت ضد اکسایشی اسانس آویشن با ریزپوشانی آن در نانو ذرات کیتوزان

م. قادری قهفرخی، م. برزگر، م. ع. سحری، م. ح. عزیزی

چکیده

استفاده از اسانس‌ها به عنوان نگهدارنده در صنعت غذا با مشکلاتی رو به رو است که از آن جمله می-توان به بر هم کنش با اجزای بافت ماده غذائی، حلالیت کم در فاز آبی، فراریت بالا و حساسیت به شرایط محیطی اشاره کرد. هدف از این مطالعه افزایش ثبات حرارتی و فعالیت ضد اکسایشی اسانس آویشن (TO) با ریزپوشانی آن در نانو ذرات کیتوزان (CS-NP) بود. اسانس آویشن با روش امولسیون- پیوندهای عرضی یونی در نانو ذرات کیتوزان ریزپوشانی شد و این فرآیند با طیف بینی مادون قرمز تبدیل فوریه (FT-IR) و تجزیه‌ی جرم سنجی حرارتی تائید گردید. تاثیر نسبت وزنی کیتوزان به اسانس بر کارائی ریزپوشانی، ظرفیت بارگذاری، اندازه ذرات و پتانسیل زتا نانو ذرات کیتوزان حاوی اسانس آویشن (CS-NP-TO) مورد بررسی قرار گرفت. اسانس ریزپوشانی شده در دمای بالاتری (۳۱۸–۳۲۵/۴ ° C) نسبت به اسانس آزاد (۱۷۰°C) تخریب گردید که نشان دهنده‌ی

[Downloaded from jast.modares.ac.ir on 2024-10-12]

[DOR: 20.1001.1.16807073.2016.18.7.20.0]

افزایش ثبات حرارتی اسانس آویشن پس از ریزپوشانی است. همچنین اسانس آویشن ریزپوشانی شده در نانو ذرات از فعالیت ضد اکسایشی بیشتری نسبت به اسانس آزاد برخوردار بود. فعالیت ضد اکسایشی و ثبات حرارتی بالاتر اسانس حاکی از آن است که این ذرات می‌توانند جهت رسانش اسانس آویشن در پزشکی، صنایع غذائی و خوراک دام مورد استفاده قرار بگیرند.

[Downloaded from jast.modares.ac.ir on 2024-10-12]

[DOR: 20.1001.1.16807073.2016.18.7.20.0]